PCCP

Accepted Manuscript

This is an *Accepted Manuscript*, which has been through the Royal Society of Chemistry peer review process and has been accepted for publication.

Accepted Manuscripts are published online shortly after acceptance, before technical editing, formatting and proof reading. Using this free service, authors can make their results available to the community, in citable form, before we publish the edited article. We will replace this *Accepted Manuscript* with the edited and formatted *Advance Article* as soon as it is available.

You can find more information about *Accepted Manuscripts* in the **Information for Authors**.

Please note that technical editing may introduce minor changes to the text and/or graphics, which may alter content. The journal's standard **Terms & Conditions** and the **Ethical guidelines** still apply. In no event shall the Royal Society of Chemistry be held responsible for any errors or omissions in this *Accepted Manuscript* or any consequences arising from the use of any information it contains.

Local environment of the molecules in water-DMSO mixtures, as seen from computer simulations and Voronoi polyhedra analysis

Abdenacer Idrissi,[1,*] B. Marekha,[1] M. Kiselev,[2] and Pál Jedlovszky[3,4,5,*]

[1]*Laboratoire de Spectrochimie Infrarouge et Raman (UMR CNRS A8516), Université Lille 1, Science et Technologies, 59655 Villeneuve d'Ascq Cedex, France*

[2]*Institute of Solution Chemistry of the Russian Academy of Sciences, Akademicheskaya 1, 153045 Ivanovo, Russia*
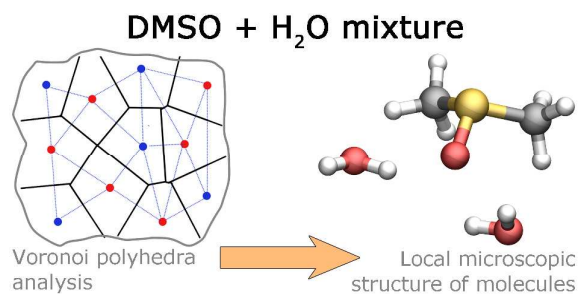
[3]*Laboratory of Interfaces and Nanosize Systems, Institute of Chemistry, Eötvös Loránd University, Pázmány P. Stny 1/A, H-1117 Budapest, Hungary*

[4]*MTA-BME Research Group of Technical Analytical Chemistry, Szt. Gellért tér 4, H-1111 Budapest, Hungary*

[5]*EKF Department of Chemistry, Leányka utca 6, H-3300 Eger, Hungary*

Running title: Voronoi analysis of water-DMSO mixtures

[*]Electronic mail: nacer.idrissi@univ-lille1.fr (A.I), pali@chem.elte.hu (P. J.)

<u>**Graphical and textual abstract for the contents page:**</u>

DMSO + H$_2$O mixture

Voronoi polyhedra analysis → Local microscopic structure of molecules

The local structure of DMSO-water mixtures is studied by computer simulation and Voronoi analysis

Abstract

Molecular dynamics simulations of water-DMSO mixtures, containing 10, 20, 30, 40, 50, 60, 70, 80, and 90 mol% DMSO, respectively, have been performed on the isothermal-isobaric (N,p,T) ensemble at $T = 298$ K and at the pressure equal to the experimental vapor pressure at each mixture composition. In addition, simulations of the two neat systems have also been performed for reference. The potential models used in the simulations are known to excellently reproduce the mixing properties of these compounds. The simulation results have been analyzed in detail by means of the Voronoi polyhedra (VP) of the molecules. Distributions of the VP volume and asphericity parameter as well as that of the radius of the spherical intermolecular voids have been calculated. Detailed analyses of these distributions have revealed that both molecules prefer to be in an environment consisting of both types of molecules, but the affinity of DMSO for mixing with water is clearly stronger than that of water for mixing with DMSO. As a consequence, the dilution of the two neat liquids by the other component has been found to follow different mechanisms: when DMSO is added to neat water small domains of neat-like water persist up to the equimolar composition, whereas no such domains are found when neat DMSO is diluted by water. The observed behavior is also in line with the fact that the main thermodynamic driving force behind the full miscibility of water and DMSO is the energy change accompanying their mixing, and that the entropy change accompanying this mixing is negative in systems of low, and positive in systems of high DMSO mole fractions. Finally, we have found a direct evidence for the existence of strong hydrogen bonded complexes formed by one DMSO and two water molecules, but it has also been shown that these complexes are in equilibrium with single (monomeric) water and DMSO molecules in the mixed systems.

1. Introduction

The study of the structure of DMSO-water mixture is highly relevant to a broad range of topics since this mixture is widely used in chemistry as a solvent in reaction media and as a cryoprotective agent in biology. The main feature of DMSO-water mixture is that close to the DMSO mole percentage of 30-40 % many physico-chemical properties, such as viscosity,[1,2] rotational correlation time of water,[3,4] translational diffusion,[5,6] static permittivity,[7] and thermophysical properties[8-11] have an extrema. Many experimental[12-22] and theoretical works[23-31] have been carried on this system with the main objective to explain this non-linear behaviour of the macroscopic properties of this mixture in terms of the intermolecular interactions (water-water, water-DMSO and DMSO-DMSO). In fact, there is a convergence in the literature that in the DMSO mole percentage range of 30-40 % the water-DMSO interactions due to hydrogen bonds are at maximum.[18] Indeed, DMSO:water complexes of the stoichiometry of 2:1 at high DMSO mole fraction,[24,26,30,32] as well as of 1:2,[6,8,24,26-28] 2:3,[27] and 1:3[33] at low DMSO content were proposed in the literature, although the existence of the latter has also been questioned.[27] However, such complexes were rather scarcely observed directly, e.g., through a detailed multiparticle spatial distribution analysis,[27] instead, their existence was merely hypothesized in explaining anomalous dynamical and thermodynamic properties of the mixture and other experimental data, or concluded on the basis of indirect evidences, such as radial distribution functions.[7,24-26] Moreover, the extent of such complexes is also a point that is far from being clarified yet: several authors assume that water-DMSO systems can be regarded as an equilibrium mixture of different species, including single water and DMSO molecules as well as complexes of different stoichiometry and even molecules interconnected in network-like fashion,[26,27] whereas others claim that complexes of certain stoichiometry involve all the water or DMSO molecules present in the system.[7] Furthermore, Kaatze et al. even concluded from the analysis of the ultrasonic absorption coefficient and the sound velocity in the DMSO-water mixtures that these systems seem to be homogenous hydrogen bonded networks rather than being composed of definite molecular complexes.[34]

These results stress the importance of the consideration of the strong hydrogen bonding interactions between DMSO and water as a characteristic feature of this mixture, as a comparison with these interactions in, e.g., acetone-water, methanol-water and urea-water mixtures. A careful analysis of the experimental and MD simulation results shows that drastic

changes are occurring in the physical properties of water (diffusion, rotational correlation time, hydrogen bond network relaxation of water, etc.[35-37]) upon adding a small amount of DMSO to water, while a milder effect is observed for these properties of DMSO when water is added to DMSO.

The present paper focuses on analyzing the local structure in the DMSO-water mixture using MD simulation. Indeed, besides experimental investigations of various kinds, this issue can also very efficiently investigated by computer simulation methods, since in a computer simulation a full, three-dimensional insight at the molecular level is obtained into the suitably chosen model of the system to be studied. Indeed, water-DMSO mixtures have been simulated a number of times in the past decades.[24-27,29-32,37] However, the reliability of the simulation results clearly depends on how well the chosen model can reproduce various experimental properties of the system of interest. From our point of view, clearly the reproduction of the mixing properties of the two compounds is of key importance. Recently, we have made a detailed comparison of the mixture of four water and eight DMSO models, and it has been found that the combination of the DMSO model proposed by Vishnyakov, Lyubartsev and Laaksonen[27] (referred to as the VLL model) and the TIP4P water model[38] is particularly successful in reproducing the thermodynamic changes accompanying the mixing of these compounds.[31] Thus, among all model combinations considered, VLL-TIP4P turned out to be clearly the best one in reproducing simultaneously the energy and entropy of mixing of the two components over the entire composition range.[31] It has also been found that the mixing of the two components is of energetic origin, as the main thermodynamic driving force behind their full miscibility is the corresponding decrease of the internal energy of the system, while the entropy change accompanying their mixing is negative, at least at low DMSO mole fractions.[31]

Having in hand a model pair that reliably describes the mixing of water and DMSO, the microscopic structure of their mixture and the local environment of the molecules in such mixtures can be very efficiently studied by Voronoi analysis.[39-41] In a three dimensional assembly of seeds, the Voronoi polyhedron (VP) of a given seed is the locus of spatial points that are closer to this seed than to any other one. (In our case, the positions of the water and DMSO molecules are regarded as the seeds.) According to this definition, the volume of a VP is a measure of the free volume available for its central seed (molecule), and, conversely, the reciprocal VP volume is a measure of the local density around this molecule. Similarly, the shape of the VP can characterize the local environment of the corresponding molecule. Further, it is clear that the faces, edges and vertices of a VP are the loci of points that are

equally close to two, three, and four seeds (molecules), respectively, and are closer to these seeds than to any other one. As a consequence, VP vertices are the spatial points at which the distance of the closest seed (molecule) is of maximum. Therefore, VP vertices mark the centers of the largest spherical vacancies between the molecules.

In this paper we present a detailed Voronoi analysis of water-DMSO mixtures of various compositions, covering the entire composition range from neat water to neat DMSO. Based on the distributions of the VP size and shape and that of the radius of the spherical voids in the system, we address the questions of whether like molecules are forming self-associates in these mixtures, how similar or different are the mechanisms of dilution of the two neat liquids by the other component, whether there is any evidence of the existence and extent of the conjectured hydrogen bonding complex DMSO•$2H_2O$ in these mixtures, and relate the results to the aforementioned fact that the mixing of water and DMSO is of energetic origin.

The paper is organized as follows. In sec. 2 details of the calculations performed, including molecular dynamics simulations and Voronoi analysis are given. The results are presented and discussed in detail in sec. 3. Finally, in sec. 4 the main conclusions of this study are summarized.

2. Computational details

2.1. Molecular dynamics simulations

Molecular dynamics simulations of water-DMSO mixtures of 11 different compositions have been performed on the isothermal-isobaric (N,p,T) ensemble at $T = 298$ K and at the pressure equal to the experimental vapor pressure at each mixture composition.[42] The basic simulation box has consisted of 864 molecules, among which 0%, 10%, 20%, 30%, 40%, 50%, 60%, 70%, 80%, 90%, and 100% have been DMSO, respectively, in the systems of different compositions. Water and DMSO molecules have been described by the rigid TIP4P and VLL potential models, respectively, as this model combination turned out to be able to very accurately describe the mixing properties of these compounds. This way, the CH_3 groups of the DMSO molecules have been treated as united atoms. According to these potential models, the total potential energy of the system has been described as the sum of the interaction energies of all molecule pairs, and the interaction energy u_{ij} of the molecule pair i

and j has been calculated as the sum of the Lennard-Jones and charge-charge Coulombic interactions of all pairs of their interaction sites:

$$u_{ij} = \sum_a^{N_i} \sum_b^{N_j} \frac{1}{4\pi \in_0} \frac{q_a q_b}{r_{ia,jb}} + 4\varepsilon_{ab} \left[\left(\frac{\sigma_{ab}}{r_{ia,jb}} \right)^{12} - \left(\frac{\sigma_{ab}}{r_{ia,jb}} \right)^6 \right] \tag{1}$$

In this equation indices a and b run over the N_i and N_j interaction sites of molecule i and j, respectively, q_a and q_b are the fractional charges carried by site a of molecule i and site b of molecule j, respectively, $r_{ia,jb}$ is the distance of these sites, σ_{ab} and ε_{ab} are the Lennard-Jones distance and energy parameters, respectively, corresponding to the site pair a and b, related to the values corresponding to the individual sites through the Lorentz-Berthelot rule:[43]

$$\sigma_{ab} = \frac{\sigma_a + \sigma_b}{2} \tag{2}$$

and

$$\varepsilon_{ab} = \sqrt{\varepsilon_a \varepsilon_b} , \tag{3}$$

and $\in_0$ is the vacuum permittivity. The interaction parameters corresponding to the two molecular models used are summarized in Table 1. All interactions have been truncated to zero beyond the center-center based cut-off distance of 14 Å. The long range part of the electrostatic interaction has been taken into account using the method of Ewald summation.[43-45]

The simulations have been performed using the DL_POLY program.[46] The temperature and pressure of the systems have been kept constant by means of the weak coupling algorithms of Berendsen et al.[47] Equations of motion have been integrated using the leap-frog algorithm, with an integration time step of 0.2 fs. Systems have been equilibrated for 5 ns. Then, in the 0.6 ns long production stage of the simulations 100000 sample configurations per system, separated by 60 fs long trajectories each, have been dumped for the analyses.

2.2. Voronoi analysis

In performing the Voronoi analysis and determining the VP around each molecule the algorithm proposed by Ruocco et al.[48] has been used. For this analysis, the positions of the water and DMSO molecules have been described by those of their O and S atoms, respectively. To calculate the volume of the VP of a given molecule, first the vertices pertaining to each face of the polyhedron have to be determined and sorted according to their sequence along the perimeter of this face.[49] The VP faces are divided to elemental triangles determined by their first, jth and $(j+1)$th vertex, and the VP itself is divided to elemental tetrahedra, one face of which being one of these elemental triangles, and the fourth vertex is the position of the molecule in the center of the VP.[49] Then, the volume of the VP, V, is calculated as the sum of the volumes of these elemental tetrahedra:

$$V = \frac{1}{6} \sum_{i=1}^{N_f} \sum_{j=2}^{n_v^{(i)}-1} \left| \left(\mathbf{r}_1^{(i)} \times \mathbf{r}_j^{(i)} \right) \cdot \mathbf{r}_{j+1}^{(i)} \right|, \tag{4}$$

N_f, $n_v^{(i)}$, and $\mathbf{r}_j^{(i)}$ being the number of faces of the VP, the number of vertices pertaining to its ith face, and the vector pointing from the molecule in the center of the VP to the jth vertex of the ith face, respectively.

To describe the shape of the VP, the asphericity parameter of Ruocco et al.,[48] η, has been used. This parameter is defined as

$$\eta = \frac{S^3}{36\pi V^2}, \tag{5}$$

S being the total surface area of the VP:

$$S = \frac{1}{2} \sum_{i=1}^{N_f} \sum_{j=2}^{n_v^{(i)}-1} \left| \left(\mathbf{r}_j^{(i)} - \mathbf{r}_1^{(i)} \right) \times \left(\mathbf{r}_{j+1}^{(i)} - \mathbf{r}_1^{(i)} \right) \right|, \tag{6}$$

calculated simply as the sum of the area of the aforementioned elemental triangles of all faces. The value of the asphericity parameter, η, is 1 for a perfect sphere, and the larger its value is the more the shape of the corresponding object deviates from the spherical one.

Finally, the radius of a spherical vacancy, R, defined by a given vertex of a VP has simply been calculated as the length of the vector pointing from this vertex to the position of the molecule inside the VP.

3. Results and discussion

3.1. Radial distribution functions

Although the main goal of the present study is to analyze the local structure of the water and DMSO molecules in their binary mixtures by means of Voronoi analysis, for completeness, and for comparisons with earlier studies, first we present a short analysis of the oxygen-oxygen radial distribution functions of different molecule pairs. The radial distribution functions corresponding to the water-water, water-DMSO and DMSO-DMSO pairs are shown in Figure 1 as obtained in the systems of different compositions simulated. The obtained radial distribution functions are in a good agreement with those published previously in the literature,[24-27] giving us therefore some additional confidence in the obtained results. As is seen, with increasing DMSO content the first peak of the water-water $g_{OO}(r)$ function gets higher, the minimum following this peak becomes deeper, the second peak around 4.5 Å gradually disappears, and a new peak around 7.5 Å emerges. These findings show, in accordance with earlier works[25,27] that in the presence of increasing amount of DMSO water-water hydrogen bonding becomes stronger, the fraction of the interstitial neighbours decreases, and the tetrahedral hydrogen bonding water network gradually breaks up. This strengthening of the water-water hydrogen bonds in the presence of DMSO was also concluded by Mancera et al from the temperature dependence of the properties of a dilute DMSO solution.[50] With increasing DMSO mole fraction even the water-DMSO $g_{OO}(r)$ function becomes more structured, its first peak gets higher and a second peak emerges around 5.5 Å, indicating, in accordance with earlier claims,[24,27,28] that even water-DMSO hydrogen bonding becomes stronger with increasing DMSO content. Finally, the comparison of the DMSO-DMSO oxygen-oxygen radial distribution function also becomes more structured as the DMSO mole fraction is increased.

3.2. Voronoi polyhedra

3.2.1. Volume distribution. The volume distributions of the Voronoi polyhedra, $P(V)$, are shown in Figure 2 as obtained in all the systems simulated. In the two neat systems the

9

$P(V)$ distribution is of Gaussian shape, as expected in systems lacking in large density fluctuations.[51] However, in the mixed systems the $P(V)$ distributions are of rather complicated shape. Thus, with increasing DMSO content the peak around 30 Å^3, observed at 0% DMSO content, first broadens to larger volumes, and then a new peak emerges around 40 Å^3. Although this peak is already the main feature of the $P(V)$ distribution at 30% DMSO content, remains of the first peak are visible up to the DMSO content of 50-60%. Further, at the high volume side of the peak around 40 Å^3 the rise of a third peak around 80 Å^3 can also be observed at 30% DMSO content. Further increase of the DMSO mole fraction leads to the rise of the latter, and a simultaneous decrease of the former peak. Thus, in the 60% DMSO system the two peaks are roughly of equal heights and above this DMSO concentration the third peak becomes already the dominant feature of the $P(V)$ distribution, while the second peak gradually vanishes, and disappears completely at 90% DMSO content. Finally, from the DMSO mole percentage of 70% a fourth peak emerges around 120 Å^3, which remains the only peak of the distribution in neat DMSO. This behavior is in a marked contrast with what was observed in other binary systems, such as mixtures of water and urea[49,52] or methanol and acetone,[52] where the $P(V)$ distribution was always found to be bimodal with no considerable composition dependence of the two peak positions. In other words, the two peaks always appeared at the positions corresponding to the two neat systems,[52] and only their relative heights changed with varying composition.

To further investigate their behavior, we tried to fit the obtained $P(V)$ curves by a sum of several Gaussian functions. In accordance with the main finding of the above visual analysis, namely that with varying composition the volume distributions exhibit peaks at four markedly different positions, some of the obtained $P(V)$ curves could only be well fitted by the sum of four Gaussians, while the use of only three Gaussians in the fit always left some features of the distributions unreproduced. This is illustrated in Figure 3, showing the fit of the $P(V)$ data obtained in the equimolar system both by the sum of three and four Gaussian functions.

The composition dependence of the peak position, V_{peak}, of the individual Gaussians contributing to the fitted function as well as that of their relative contribution to the fitted function (i.e., their weight in their sum), w_{peak}, are shown in Figure 4. In accordance with the above findings, the positions of the four peaks are always well separated from each other, indicating that they correspond to molecules of markedly different local environments. Clearly, the first and fourth peaks are given by such water and DMSO molecules, respectively, which are surrounded by like neighbors in all directions, and hence feel

10

themselves in a similar local environment as in their neat liquids. Consistently with this interpretation, the positions of these peaks do not depend considerably on the composition of the system, and the weight of the first peak decreases, while that of the fourth peak increases sharply with increasing DMSO concentration. Clearly, the less molecules of the other type are in the system, the more molecules of the major component find themselves in a neat-like local environment.

The second and third peaks of the $P(V)$ distributions can, on the other hand, be attributed to water and DMSO molecules, respectively, which are in a mixed local environment formed by both water and DMSO molecules. Clearly, the aforementioned difference between the set of $P(V)$ distributions obtained here and those obtained previously in methanol-acetone mixtures.[52] As it was shown previously, the miscibility of water and DMSO is of energetic origin, i.e., the excess energy accompanying their mixing is negative.[31] On the other hand, the mixing of methanol and acetone is driven by the increase of the entropy, while the energy change corresponding to this mixing is positive.[53] As a consequence, methanol and acetone exhibit microscopic separation (self-association) in their mixtures,[52,53] whereas water and DMSO mix with each other even on the molecular scale.[31] This difference in the thermodynamic background of the mixing of these components is reflected in the differences of their $P(V)$ distributions. Thus, due to the strong self-association behavior, in methanol-acetone mixtures the majority of both molecules find themselves in a locally neat-like environment, i.e., surrounded by like molecules, which leads to the prevalence of the peaks corresponding to the two neat liquids over the entire composition range. On the other hand, in water-DMSO mixtures the molecules prefer to be surrounded by unlike neighbors, and hence the two peaks corresponding to the two kinds of molecules being in mixed environment appear in the $P(V)$ distribution, and dominate it over a very broad range of compositions. The facts that both of these peaks are contributing to the $P(V)$ distribution in all the mixed systems considered, from 10 to 90% DMSO content, and that one of them is the dominant feature of the $P(V)$ distribution from 20 to 70% DMSO content (see Fig. 4) demonstrate the extent and importance of this molecular scale mixing in water-DMSO mixtures. However, the fact that the first peak, corresponding to water in aqueous environment, is present over a considerably broader composition range than the fourth peak (i.e., DMSO surrounded by other DMSO molecules) suggests that the dilution of the two neat systems might correspond to somewhat different molecular mechanisms, i.e., the aforementioned affinity of the water and DMSO

molecules for being mixed with each other might not have the same extent. This point is addressed in detail in the following sub-section.

It should also be noted that the aforementioned molecular scale mixing of water and DMSO is in a full accordance with a number of previous experimental[13,17] and computer simulation studies,[24-27,31] and it is also compatible with the assumption[7,13,24-27,54,55] that two water and one DMSO molecules can form a particularly strong hydrogen bonded complex, often referred to as DMSO•2H$_2$O. Although the present results can well be compatible with such a picture, solely on the basis of the VP volume distribution analysis we cannot yet prove or falsify this assumption. Nevertheless, it is clear that, contrary to some recent claims,[7] even if such complexes are present in mixtures of water and DMSO, they by no means involve all the water or DMSO molecules in the system. If the system could be regarded as a simple ternary mixture of water and DMSO molecules and of DMSO•2H$_2$O complexes (in other words, water and DMSO molecules being in mixed environment would always be parts of such complexes), the weight of the second peak of the $P(V)$ distribution would always be the double of that of the third one (as these weights are proportional to the number of water and DMSO molecules, respectively, being in mixed environment). It can also be excluded that in the stoichiometric mixture of 33% DMSO and 67% water all the molecules would be involved in such complexes, as the contribution of the second peak is roughly equal to that of the third peak rather than being about twice as large both in the 30% and 40% DMSO system, being closest to the stoichiometric composition. Instead, the obtained results indicate that the term 'mixed environment' of the molecules means much more than simply the presence of DMSO•2H$_2$O complexes; such a mixed environment can correspond to a large variety of local arrangements of DMSO and water molecules of various fractions around the central molecule. This view is also consistent with the fact that, unlike in the case of the first and fourth peak, corresponding to always very similar local environments, the positions of the second and third peaks show non-negligible composition dependence (see Fig. 4), reflecting the above change of the mixed local environment with the composition of the system. The question of the possible presence of DMSO•2H$_2$O hydrogen bonded complexes in the systems will be further addressed in the following sub-section.

To demonstrate once more the lack of large self-associates in water-DMSO mixtures we have also calculated the VP volume distributions by disregarding one component and taking solely the other one in the analysis. As it was demonstrated by Zaninetti more than two decades ago, the VP volume distribution of uniformly distributed points is of Gaussian shape, whereas in the case of large density fluctuations (i.e., strong correlation between the positions

of the points) the VP volume distribution develops a long, exponentially decaying tail at the large volume side of its peak.[51] Hence, in case of self-association of the components in binary mixtures, i.e., when both individual components show inhomogeneous density distribution, the $P(V)$ distribution obtained by disregarding on of the two components exhibits the exponentially decaying tail (as in this case the self-associates of the disregarded component are transformed to empty regions in the system).[49] On the other hand, in the lack of such self-association the VP volume distribution remains of Gaussian shape even when one of the two components is disregarded in the analysis.

Figure 5 shows the $P(V)$ distributions obtained both by taking both components into account and by disregarding one of them. To better demonstrate the lack of their exponentially decaying tail at high volumes, the distributions are shown on a logarithmic scale. As is seen, the decay of the distributions at large volumes is never exponential (i.e., never transformed to linear decay on the used logarithmic scale), again in a marked contrast with our previous results on methanol-acetone mixtures (see Fig. 1 of Ref. 52). It is also seen, however, that the large V decay of the $P(V)$ curve obtained in the 10% DMSO system when water molecules have been disregarded (middle panel in Figure 5) is considerably closer to the exponential one (i.e., linear on the used logarithmic scale) than that obtained in the 90% DMSO system by disregarding the DMSO molecules (bottom panel in Figure 5). This finding suggests again that, among the two molecules, DMSO has a stronger affinity for mixing with unlike molecules in these systems than water. This point is further discussed in the following sub-section.

3.2.2. Asphericity

The distribution of the asphericity parameter of the VP, η, defined by eq. 5 is shown in Figure 6 as obtained in the different systems simulated. As is seen, similarly to $P(V)$, the asphericity parameter distributions in the mixed systems are also of rather complex shape. In neat water the $P(\eta)$ curve is of Gaussian shape, centered at the η value of 1.64. In the presence of DMSO another peak, located around 1.9 contributes also to the $P(\eta)$ distribution (although at certain compositions it only appears as a shoulder). The peak at low η values, however, does not vanish with increasing DMSO concentration, instead, it broadens (up to about 70% DMSO content), then gradually shifts to lower asphericity values, and remains the single peak, located at the η value of 1.50, in neat DMSO. Simultaneously, the high asphericity peak, which increases up to 30% DMSO content, starts to decrease upon further

13

increasing the DMSO mole fraction, and finally vanishes in neat DMSO. This behavior is again in a marked contrast with what was observed in methanol-acetone mixtures, where, similarly to $P(V)$, the $P(\eta)$ distributions also turned out to be bimodal with no dependence of the peak positions on the composition (see Fig. 8 of Ref. 52).

Although the $P(\eta)$ distribution looks bimodal in all the mixed systems, our attempt to fit them by the sum of two Gaussian functions always left some of their parts unfitted, whereas very good fit was always obtained by the sum of three Gaussian functions. This is illustrated in Figure 7, showing the fitting of the $P(\eta)$ distribution corresponding to the equimolar system by the sums of two and three Gaussian functions. The variation of the peak position of the three Gaussian functions, η_{peak}, as well as that of their relative contributions to the sum are shown in Figure 8.

As is seen, the positions of none of the three peaks varies systematically with the composition, instead, they are more or less constant over the entire composition range in which they contribute considerably to the fitting function. The small shifts of the peak positions can simply be attributed to the increasing numerical inaccuracy of their determination in the fitting procedure when the contribution of the corresponding peak becomes too small. It is also seen that the contribution of the lowest η peak increases continuously from 0 to 1, while that of the peak at intermediate η value decreases from 1 to 0 with increasing DMSO mole fraction. (The increase of the contribution of the second peak between the DMSO mole percentage values of 40 and 70% can again be explained by the numerical instability of the fit, considering that these two peaks, having comparable weights in this composition range, are located rather close to each other.) Clearly, the first (i.e., lowest η) peak corresponds to DMSO molecules that are surrounded by other DMSO molecules, while the second one corresponds to water molecules that are surrounded by other waters. It is not surprising that the local environment of the former molecules is more spherical than that of the latter ones, considering the fact that the first coordination shell of a DMSO molecule in the neat liquid consists of 12 nearest neighbors, while water is only tetrahedrally coordinated.

The third, large η peak, present in all mixed systems considered is given by molecules in mixed local environment. The contribution of this peak to the $P(\eta)$ distribution increases up to 40% DMSO content, and decreases upon further increase of the DMSO mole fraction in the system. Again, it is not surprising that molecules having both water and DMSO neighbors are in a less spherical local environment than those being surrounded by like neighbors only. It is interesting, however, that the asphericity parameter corresponding to the water and DMSO

14

molecules that are located in mixed environment does not differ noticeably from each other. This finding emphasizes that, unlike the volume of the VP, which evidently depends on the size of the central molecule, the asphericity parameter reflects the properties of solely the local environment and not that of the central molecule. Hence, the sphericity of the local environment formed by the mixture of water and DMSO molecules does not depend on whether the central molecule in this environment is water or DMSO.

The conclusions drawn from the analysis of the asphericity parameter distributions are in line with those obtained from the analysis of the VP volume distributions, and stress again the strong preference of the two molecules to mix with each other even on the molecular scale.

3.3. Intermolecular voids

The distributions of the radius R of the spherical vacancies in the systems simulated are shown in Figure 9. At the first sight, these distributions look considerably simpler than either those of the VP volume or VP asphericity. Thus, in neat water $P(R)$ is of Gaussian shape centered at $R = 2.46$ Å. Upon increasing the DMSO mole fraction, this peak gradually decreases, turns into a shoulder in the 30% DMSO system, and vanishes above 70% DMSO content. Simultaneously, a second peak emerges at higher R values, which increases with increasing DMSO mole fraction, and becomes the only feature of the $P(R)$ distribution above 70% DMSO content. Interestingly, the position of the first peak seems to be insensitive to the composition of the system, while the second peak gradually shifts to larger R values with increasing DMSO mole fraction. Nevertheless, the $P(R)$ distributions can always be very well fitted by the sum of only two Gaussian functions, as illustrated in the inset of Fig. 9 on the example of the 20% DMSO system. It should also be noted that the obtained $P(R)$ distributions differ again considerably from what was seen in methanol-acetone mixtures,[52] where the distribution turned out to be of a simple Gaussian shape at any composition, and only the peak of the Gaussian shifted gradually with changing composition (see Fig. 6 of Ref. 52).

The dependence of the position of the two Gaussians and of their relative contributions to the fitting function of the $P(R)$ data on the composition of the system are shown on Figure 10. This figure clearly confirms our above observation that the first peak appears always at the same position of about 2.45 Å, whereas the second peak shifts gradually to larger R values from about 3.0 Å to 3.8 Å. The contributions of the two peaks become roughly equal already

15

in the 10% DMSO system, and the weight of the first peak becomes negligible around the DMSO mole percentage of 40-50%.

The different behavior of the two peaks with changing composition stresses again that the dilution of the two neat systems corresponds to different mechanisms. Since the first peak is the only feature of the $P(R)$ distribution in neat water, it corresponds to voids that are surrounded solely by water molecules. Thus, the presence of this peak in the water-rich mixtures indicates the presence of such voids, and hence that of at least small domains of neat water. The rapid decrease of the contribution of this peak to the $P(R)$ distribution is a clear sign of the rapid decrease of the number and extent of such domains with increasing DMSO mole fraction; nevertheless, such domains are noticeably present in the mixture up to at least the equimolar composition. On the other hand, no such neat DMSO domains are seen even at low water concentration, as the peak characterizing the void size in neat DMSO shifts gradually to lower R values as the water content of the system is increased. Therefore, this peak marks the presence of voids surrounded by both types of molecules, and the fraction of these surrounding molecules varies smoothly with the variation of the overall composition of the system, as witnessed by the gradual shift of the peak position. In short, dilution of water by DMSO occurs by preserving neat-water-like domains in the system at least as long as water is the major component, whereas dilution of DMSO by water occurs in a different way, by forming uniform mixture of the two molecules even on the molecular scale. This finding is also consistent with the fact that at low DMSO mole fractions the entropy of mixing of the two components is negative (and, hence, from the entropic point of view formation of neat-like water domains is favorable), whereas at high DMSO mole fractions the entropy of mixing is positive (and therefore the formation of neat-like DMSO domains is unfavorable even in this respect).[31]] This result highlights the general conclusion that the affinity of the two molecules for mixing with each other is different: this affinity of DMSO for mixing with water is clearly stronger than that of water for mixing with DMSO.

This finding can be further elaborated by calculating the $P(R)$ distribution in the systems of different compositions by disregarding one of the two components in the analysis. As it has been pointed out in a previous sub-section, this way self-associates of the disregarded component are transformed to voids, the radius of which will thus contribute to the $P(R)$ distribution of the other component. The $P(R)$ curves obtained by taking only the DMSO molecules into account and disregarding waters and by taking only the water molecules into account and disregarding DMSO are shown in Figures 11 and 12, respectively. As is seen, the two sets of $P(R)$ curves behave in a markedly different way. Thus, the $P(R)$

16

distributions obtained for DMSO by disregarding the water molecules is always of Gaussian shape, and this Gaussian shifts rapidly to larger R values and becomes broader with decreasing DMSO mole fraction. The behaviour of this peak can simply be explained by the increasing water content: the larger is the mole fraction of the water molecules in the system the larger space they occupy, and hence the larger will be the volume of this space (transformed to voids by disregarding water molecules in the analysis) with increasing water mole fraction.

The $P(R)$ distributions obtained by disregarding the DMSO molecules and taking only waters into account (Fig. 12), on the other hand, show a considerably more complicated picture. Although these functions are usually seemingly bimodal, they can only be well fitted by the sum of at least three Gaussians (see the inset of Fig. 12). The composition dependence of the position of these Gaussians and of their relative contribution to the sum are shown in Figure 13. As is seen, the position of the first and second peaks is more or less independent on the composition, while that of the third peak increases sharply with increasing DMSO mole fraction. This peak is clearly the counterpart of the one seen when only DMSO molecules are taken into account, and can be explained simply by the trivial effect of the dilution of the system. The first peak, present with a noticeable contribution in water-rich systems and occurring always around 2.40 - 2.45 Å marks the voids that are surrounded solely by water molecules in neat-water-like environment, and hence do not change upon disregarding the DMSO molecules in the analysis. The presence of the second peak, however, cannot be explained by the previous findings.

As is seen, this peak, present in the mixed systems, appears always in the R range of 4.0 – 4.4 Å. With increasing DMSO mole fraction its contribution to the $P(R)$ distribution increases up to 30-40% DMSO content, and drops rapidly upon further increase of the DMSO mole fraction in the system. The insensitivity of the peak position to the overall composition of the system is an indication of the presence of a stable, composition independent structural element, and the fact that the contribution of this peak is the largest around 30-40% DMSO content reveals that this structural element is the DMSO•$2H_2O$ hydrogen bonded complex of one DMSO and two water molecules, the possible presence of which in the mixed systems has already been discussed in a previous sub-section. Since the occurrence of this second peak in the $P(R)$ distributions of solely the water molecules cannot be explained without the presence of such complexes in the system, this finding is a direct evidence that strong hydrogen bonded complexes of the stoichiometry of DMSO•$2H_2O$ are present in the DMSO-water mixtures simulated with the VLL-TIP4P model pair.

17

4. Summary and Conclusions

In this paper we have presented a detailed analysis of the local structure of water-DMSO mixtures of various compositions on the basis of computer simulations with a potential model pair that describes very well the mixing properties of these compounds, and Voronoi analysis. Voronoi analysis turned out to be particularly useful in revealing peculiar features of the molecular scale structure of the system. The analysis of the VP volume distributions has revealed that both molecules prefer to stay in a local environment consisting of both types of surrounding molecules. This finding is in a clear accordance with the fact that the mixing of water and DMSO is driven by the energy decrease accompanying this mixing.[31] We have also demonstrated that neither of the two molecules tend to form relatively large self-associates, in a clear contrast with entropy-driven mixtures, such as the methanol-acetone system.[52,53] Nevertheless, the affinity of the two molecules for mixing with the other one has turned out to be different: the preference of the DMSO molecules for being in contact with waters is clearly stronger than that of the water molecules for being in contact with DMSO. As a consequence, the dilution of the two neat liquids by the other component corresponds to different molecular mechanisms. Thus, when DMSO is added to neat water, small domains of neat-like water persist up to about the equimolar composition. On the other hand, when water is added to neat DMSO the two components are mixed uniformly, without the existence of small domains of different compositions (e.g., neat-like DMSO). This difference is in a clear accordance with the fact that self-association of water molecules at low DMSO mole fractions is favored at least by the entropic term corresponding to the mixing of the two neat components, whereas in systems of high DMSO mole fractions both the entropy and energy of mixing favor the molecular scale mixing of the two components.[31] All the above conclusions were also confirmed by the analysis of the distributions of the VP asphericity parameter and of the radius of the intermolecular voids.

Finally, by analyzing the size distribution of the spherical voids in the systems by disregarding DMSO molecules (i.e., converting the space they occupy also to voids) we have found a direct evidence of the presence of strongly hydrogen bonded complexes formed by one DMSO and two water molecules in the simulated systems. We have also demonstrated, however, that although such DMSO•$2H_2O$ complexes are evidently present in the system; they by no means involve all the possible water or DMSO molecules. Instead, the formation

18

and breaking of such complexes is an equilibrium process, as DMSO•2H$_2$O complexes coexist in the system at every composition with single (monomeric) water and DMSO molecules.

Acknowledgements

References

1.   S. A. Schichman and R. L. Amey, *J. Phys. Chem.*, 1971, **75**, 98.
2.   M. del Carmen Grande, J. A. Juliá, M. García and C. M. Marschoff, *J. Chem. Thermodyn.*, 2007, **39**, 1049.
3.   B. C. Gordalla and M. D. Zeidler, *Mol. Phys.*, 1986, **59**, 817.
4.   B. C. Gordalla and M. D. Zeidler, *Mol. Phys.*, 1991, **74**, 975.
5.   K. J. Packer and D. J. Tomlinson, *Trans. Faraday Soc.*, 1971, **67**, 1302.
6.   H. N. Bordallo, K. W. Herwig, B. M. Luther and N. E. Levinger, *J. Chem. Phys.*, 2004, **121**, 12457.
7.   I. Płowaś, J. Świergiel and J. Jadżyn, *J. Chem. Eng. Data.*, 2013, **58**, 1741.
8.   M. Palaiologou, G. Arianas and N. Tsierkezos, *J. Solution. Chem.*, 2006, **35**, 1551.
9.   R. B. Tôrres, A. C. M. Marchiore and P. L. O. Volpe, *J. Chem. Thermodyn.*, 2006, **38**, 526.
10. G. I. Egorov and D. M. Makarov, *Russ. J. Phys. Chem. A*, 2009, **83**, 693.

11.   V. V. Sergievskii, D. S. Skorobogat'ko and A. M. Rudakov, *Russ. J. Phys. Chem. A*, 2010, **84**, 350.

12.   A. Bertoluzza, S. Bonora, M. A. Battaglia and P. Monti, *J. Raman. Spectrosc.*, 1979, **8**, 231.

13.   A. K. Soper and A. Luzar, *J. Chem. Phys.*, 1992, **97**, 1320.

14.   D. N. Shin, J. W. Wijnen, J. B. F. N. Engberts and A. Wakisaka, *J. Phys. Chem. B*, 2001, **105**, 6759.

15.   P. P. Wiewiór, H. Shirota and E. W. Castner, *J. Chem. Phys.*, 2002, **116**, 4643.

16.   A. Wulf and R. Ludwig, *ChemPhysChem*, 2006, **7**, 266.

17.   S. E. McLain, A. K. Soper and A. Luzar, *J. Chem. Phys.*, 2007, **127**. 174515.

18.   K. Noack, J. Kiefer and A. Leipertz, *ChemPhysChem*, 2010, **11**, 630.

19.   S. L. Ouyang, N.-N. Wu, J. Y. Liu, C. L. Sun, Z. W. Li and S. Q. Gao, *Chinese Physics B*, 2010, **19**, 123101.

20.   J.-C. Jiang, K.-H. Lin, S.-C. Li, P.-M. Shih, K.-C. Hung, S. H. Lin and H.-C. Chang, *J. Chem. Phys.*, 2011, **134**, 044506.

21.   D. B. Wong, K. P. Sokolowsky, M. I. El-Barghouthi, E. E. Fenn, C. H. Giammanco, A. L. Sturlaugson and M. D. Fayer, *J. Phys. Chem. B*, 2012, **116**, 5479.

22.   M. N. Rodnikova, Y. A. Zakharova, I. A. Solonina and D. A. Sirotkin, *Russ. J. Phys. Chem. A*, 2012, **86**, 892.

23.   G. Brink and M. Falk, *J. Mol. Struct.*, 1970, **5**, 27.

24.   I. I. Vaisman and M. L. Berkowitz, *J. Am. Chem. Soc.*, 1992, **114**, 7889.

25.   A. Luzar and D. Chandler, *J. Chem. Phys.*, 1993, **98**, 8160.

26.   I. A. Borin and M. S. Skaf, *J. Chem. Phys.*, 1999, **110**, 6412.

27.   A. Vishnyakov, A. P. Lyubartsev and A. Laaksonen, *J. Phys. Chem. A*, 2001, **105**, 1702.

28.   R. L. Mancera, M. Chalaris and J. Samios, *J. Mol. Liq.*, 2004, **110**, 1473.

29.   S. Roy, S. Banerjee, N. Biyani, B. Jana and B. Bagchi, *J. Phys. Chem. B*, 2010, **115**, 685.

30.   N. Zhang, W. Li, C. Chen and J. Zuo, *Comput. Theor. Chem.*, 2013, **1017**, 126.

31.   A. Idrissi, B. Marekha, M. Barj and P. Jedlovszky, *J. Phys. Chem. B*, 2014, **118**, 8724.

32.   Q. Zhang, X. Zhang and D.-X. Zhao, *J. Mol. Liq.*, 2009, **145**, 67.

33.   B. Kirchner and J. Hutter, *Chem. Phys. Lett.*, 2002, **364**, 497.

34.   U. Kaatze, M. Brai, F. D. Scholle and R. Pottel, *J. Mol. Liq.*, 1990, **44**, 197.

35.   C. Nieto-Draghi, J. Bonet Ávalos and B. Rousseau, *J. Chem. Phys.*, 2003, **119**, 4782.

36. N. Engel, K. Atak, K. M. Lange, M. Gotz, M. Soldatov, R. Golnak, E. Suljoti, J.-E. Rubensson and E. F. Aziz, *J. Phys. Chem. Lett.*, 2012, **3**, 3697.

37. S. Chowdhuri and S. K. Pattanayak, *Mol. Phys.*, 2012, **111**, 135.

38. W. L. Jorgensen, J. Chandrasekhar, J. D. Madura, R. W. Impey and M. L. Klein, *J. Chem. Phys.*, 1983, **79**, 926.

39. G. Voronoi, *J. Reine Angew. Math.*, 1908, **1908**, 198.

40. N. N. Medvedev, *The Voronoi-Delaunay Method in Srtuctural Studies of Noncrystalline Systems*, SB RAS, Novosibirsk, 2000.

41. A. Okabe, B. Boots, K. Sugihara and S. N. Chiu, *Spatial Tessellations: Concepts and Applications of Voronoi Diagrams*, John Wiley & Sons, Inc., Chichester, 2000.

42. X. Qian, B. Han, Y. Liu, H. Yan and R. Liu, *J. Solution. Chem.*, 1995, **24**, 1183.

43. P. Allen and D. J. Tildesley, *Computer simulation of liquids*, Clarendon Press, Oxford, 1987.

44. P. P. Ewald, *Ann, Phys.*, 1921, **369**, 253.

45. S. W. de Leeuw, J. W. Perram and E. R. Smith, *Proc. R. Soc. London, Ser. A*, 1980, **373**, 27.

46. W. Smith and T. R. Forester, *J. Mol. Graph.*, 1996, **14**, 136.

47. H. J. C. Berendsen, J. P. M. Postma, W. F. van Gunsteren, A. DiNola and J. R. Haak, *J. Chem. Phys.*, 1984, **81**, 3684.

48. G. Ruocco, M. Sampoli and R. Vallauri, *J. Chem. Phys.*, 1992, **96**, 6167.

49. A. Idrissi, P. Damay, K. Yukichi and P. Jedlovszky, *J. Chem. Phys.*, 2008, **129**, 164512.

50. R. L. Mancera, M. Chalaris, K. Refson and J. Samios, *Phys. Chem. Chem. Phys.*, 2004, **6,** 94.

51. L. Zaninetti, *Phys. Lett. A*, 1992, **165**, 143.

52. A. Idrissi, K. Polok, W. Gadomski, I. Vyalov, A. Agapov, M. Kiselev, M. Barj and P. Jedlovszky, *Phys. Chem. Chem. Phys.*, 2012, **14**, 5979.

53. A. Idrissi, K. Polok, M. Barj, B. Marekha, M. Kiselev and P. Jedlovszky, *J. Phys. Chem. B*, 2013, **117**, 16157.

54. D. H. Rasmussen, A. P. MacKenzie, *Nature* 1968, **220,** 1315.

55. J. A. Glasel, *J. Am. Chem. Soc.* **1970,** 92, 372.

Tables

Table 1. Interaction parameters of the molecular models used

molecule	interaction site	q/e	ε/kJ mol^{-1}	σ/Å
DMSO[a]	S	0.139	1.399	3.66
	C	0.160	0.096	3.76
	O	-0.459	0.591	2.92
water[b]	O	0	0.6491	3.154
	H	0.52	-	-
	M[c]	-1.04	-	-

[a]Ref. 27
[b]Ref. 38
[c]Non-atomic interaction site, placed along the H-O-H angle bisector 0.15 Å away from the O atom.

Figure legend

Fig. 1. Oxygen-oxygen radial distribution functions corresponding to two water molecules (top panel), a water and a DMSO molecule (middle panel), and two DMSO molecules (bottom panel) in the systems of different compositions simulated. Arrows indicate the order of the obtained functions in the direction of increasing DMSO mole percentage.

Fig. 2. Distribution of the volume of the VP of the molecules in water-DMSO mixtures of different compositions. The distributions obtained in the systems containing 90%, 80%, 70%, 60%, 50%, 40%, 30%, 20%, 10%, and 0% DMSO are shifted upwards by 0.01, 0.02, 0.03, 0.04, 0.05, 0.06, 0.07, 0.08, 0.09 and 0.1 units, respectively, for clarity.

Fig. 3. Fitting the VP volume distribution of the equimolar system by the sum of three (top panel) and four (bottom panel) Gaussian functions. The simulated $P(V)$ data are shown by black filled circles, the individual Gaussians by dashed blue lines, and their sums by solid red lines. The inset shows a part of the simulated function and of the fit with three Gaussians on a magnified scale.

Fig. 4. Composition dependence of the peak positions of the individual Gaussian functions the sum of which fits the simulated $P(V)$ data (top panel) and the relative contribution of these Gaussian peaks to their sum (bottom panel). The lines connecting the points are just guides to the eye.

Fig. 5. VP volume distribution in water-DMSO mixtures containing 10% (black squares), 30% (red circles), 50% (green up triangles), 70% (dark blue down triangles) and 90% (light blue diamonds) DMSO, calculated by taking all molecules into account (top panel), taking only the DMSO molecules into account and disregarding waters (middle panel), and taking only water molecules into account and disregarding DMSO (bottom panel) in the analysis. To better demonstrate the non-linear decay of the peaks, the distributions are shown on a semi-logarithmic scale.

Fig. 6. Distribution of the asphericity parameter of the VP of the molecules in water-DMSO mixtures of different compositions. The distributions obtained in the systems containing 90%, 80%, 70%, 60%, 50%, 40%, 30%, 20%, 10%, and 0% DMSO are shifted upwards by 0.025, 0.05, 0.075, 0.1, 0.125, 0.15, 0.175, 0.2, 0.225 and 0.25 units, respectively, for clarity.

Fig. 7. Fitting the VP asphericity parameter distribution of the equimolar system by the sum of two (top panel) and three (bottom panel) Gaussian functions. The simulated $P(\eta)$ data are shown by black filled circles, the individual Gaussians by dashed blue lines, and their sums by solid red lines. The inset shows a part of the simulated function and of the fit with two Gaussians on a magnified scale.

Fig. 8. Composition dependence of the peak positions of the individual Gaussian functions the sum of which fits the simulated $P(\eta)$ data (top panel) and the relative contribution of these Gaussian peaks to their sum (bottom panel). The lines connecting the points are just guides to the eye.

Fig. 9. Distribution of the radius of the spherical voids between the molecules in water-DMSO mixtures of different compositions. The distributions obtained in the systems containing 90%, 80%, 70%, 60%, 50%, 40%, 30%, 20%, 10%, and 0% DMSO are shifted upwards by 0.015, 0.03, 0.045, 0.6, 0.075, 0.09, 0.105, 0.12, 0.135 and 0.15 units, respectively, for clarity. The inset shows the fit of the simulated $P(R)$ data (black filled circles) by the sum of two Gaussian functions. The individual Gaussian functions and their sum are shown by dashed blue lines and a solid red line, respectively.

Fig. 10. Composition dependence of the peak positions of the individual Gaussian functions the sum of which fits the simulated $P(R)$ data (top panel) and the relative contribution of these Gaussian peaks to their sum (bottom panel). The lines connecting the points are just guides to the eye.

24

Fig. 11. Distribution of the radius of the spherical voids between the molecules in water-DMSO mixtures of different compositions, obtained by taking into account only the DMSO molecules, and disregarding waters in the analysis. The distributions obtained in the systems containing 90%, 80%, 70%, 60%, 50%, 40%, 30%, 20%, and 10%, DMSO are shifted upwards by 0.015, 0.03, 0.045, 0.6, 0.075, 0.09, 0.105, 0.12, and 0.135 units, respectively, for clarity.

Fig. 12. Distribution of the radius of the spherical voids between the molecules in water-DMSO mixtures of different compositions, obtained by taking into account only the water molecules, and disregarding DMSO in the analysis. The distributions obtained in the systems containing 80%, 70%, 60%, 50%, 40%, 30%, 20%, 10%, and 0% DMSO are shifted upwards by 0.011, 0.022, 0.033, 0.44, 0.055, 0.066, 0.077, 0.088, and 0.11 units, respectively, for clarity. The inset shows the fit of the simulated $P(R)$ data (black filled circles) by the sum of three Gaussian functions. The individual Gaussian functions and their sum are shown by dashed blue lines and a solid red line, respectively.

Fig. 13. Composition dependence of the peak positions of the individual Gaussian functions, the sum of which fits the simulated $P(R)$ data obtained by disregarding DMSO and taking only water molecules into account in the analysis, (top panel) and the relative contribution of these Gaussian peaks to their sum (bottom panel). The inset shows the composition dependence of the peak positions of the single Gaussian function that fits the simulated $P(R)$ data obtained by disregarding waters and taking only DMSO molecules into account in the analysis. The solid lines connecting the points are just guides to the eye.
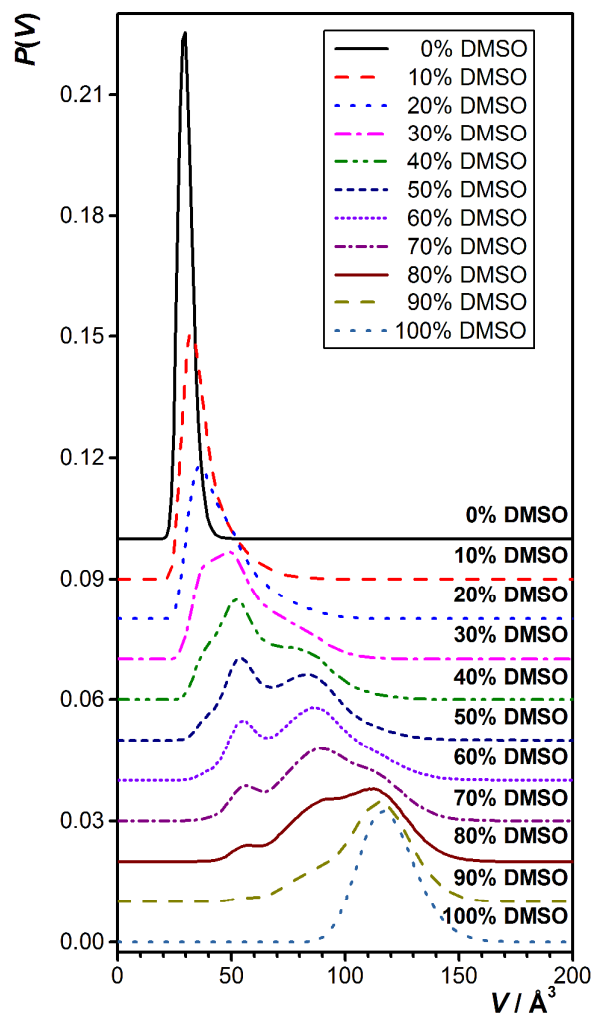
Figure 1.

Idrissi et al.
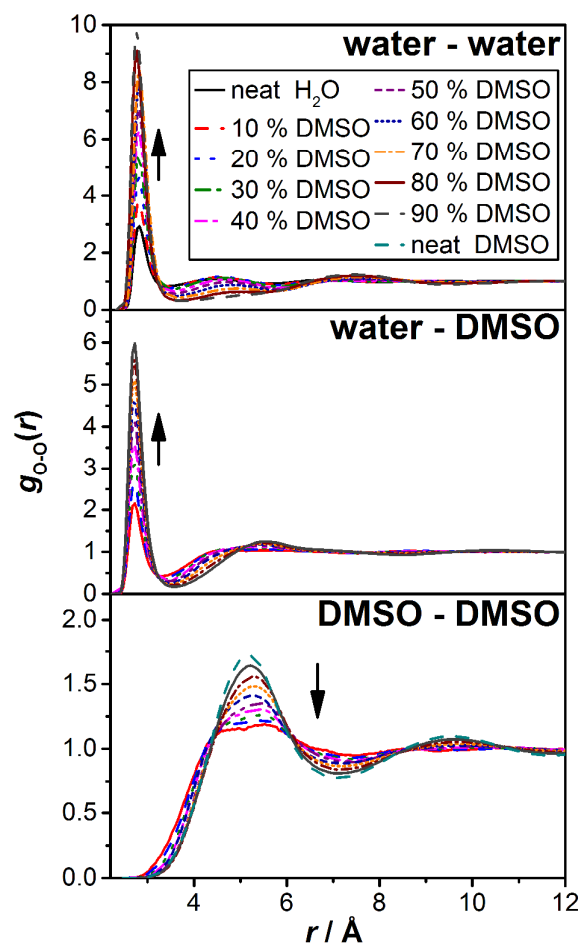
Figure 2.
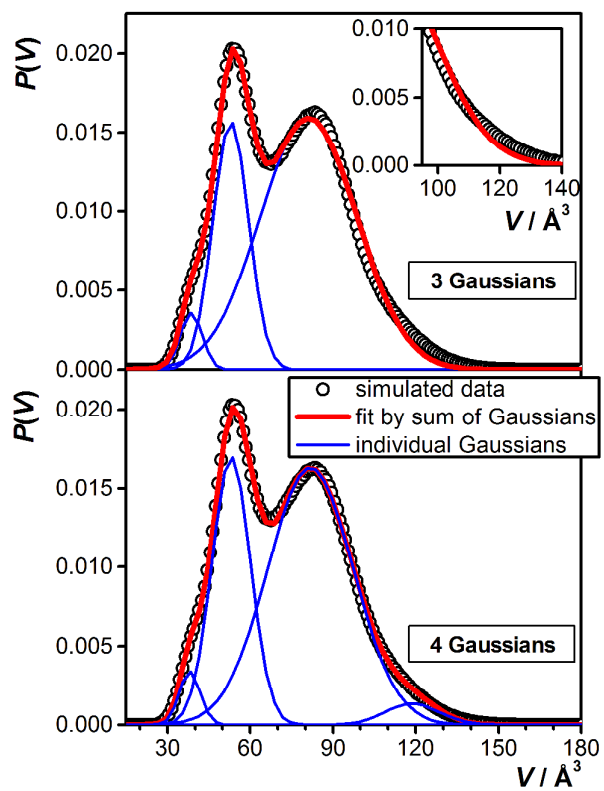
Idrissi et al.

Figure 3.

Idrissi et al.

Figure 4.

Idrissi et al.
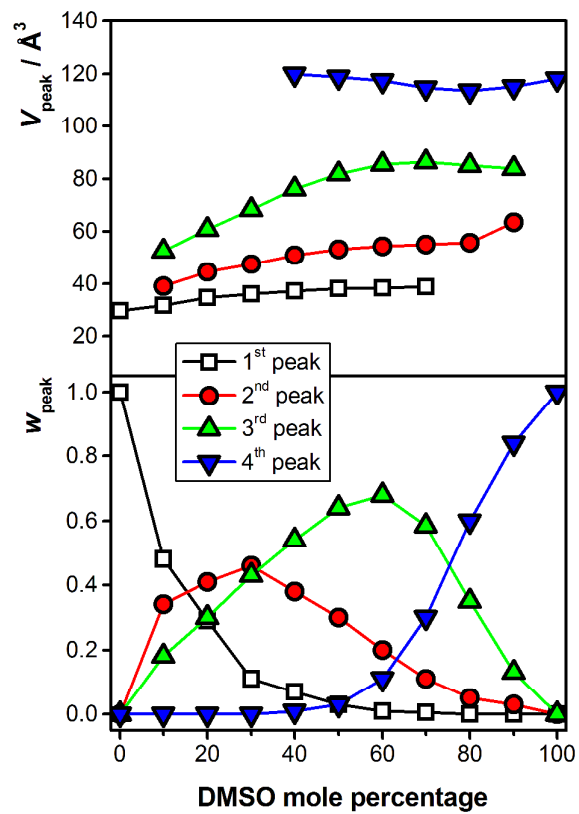
Figure 5.

Idrissi et al.
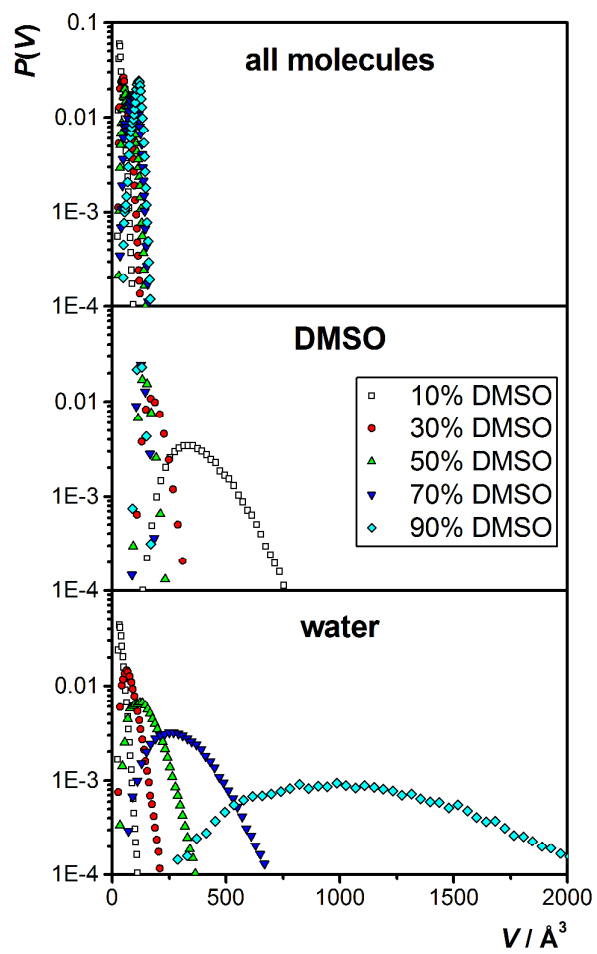
Figure 6.

Idrissi et al.
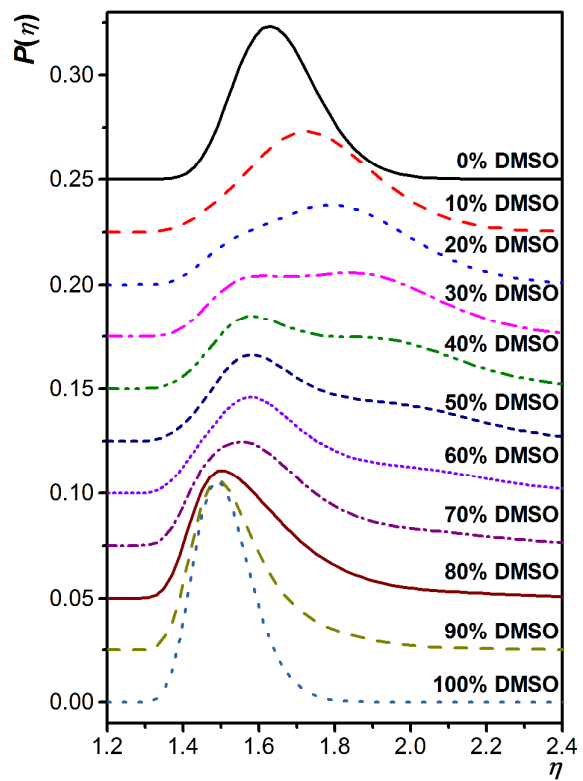
Figure 7.

Idrissi et al.
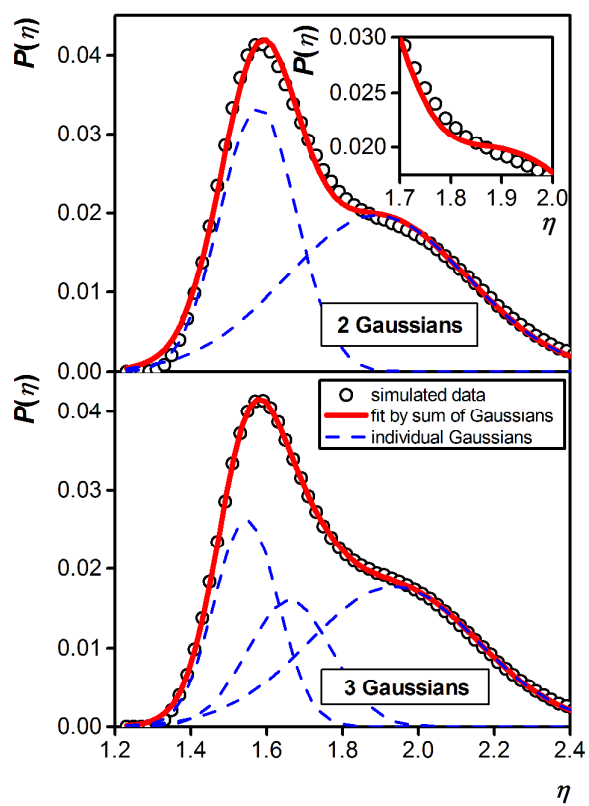
Figure 8.

Idrissi et al.
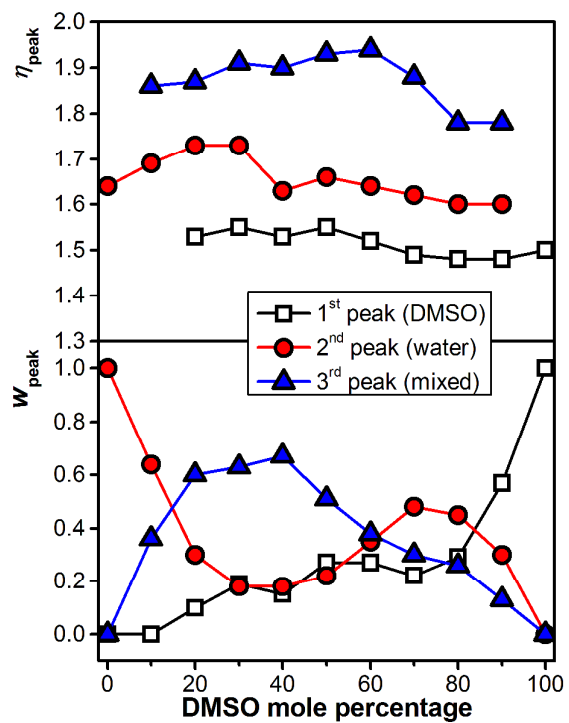
Figure 9.

Idrissi et al.
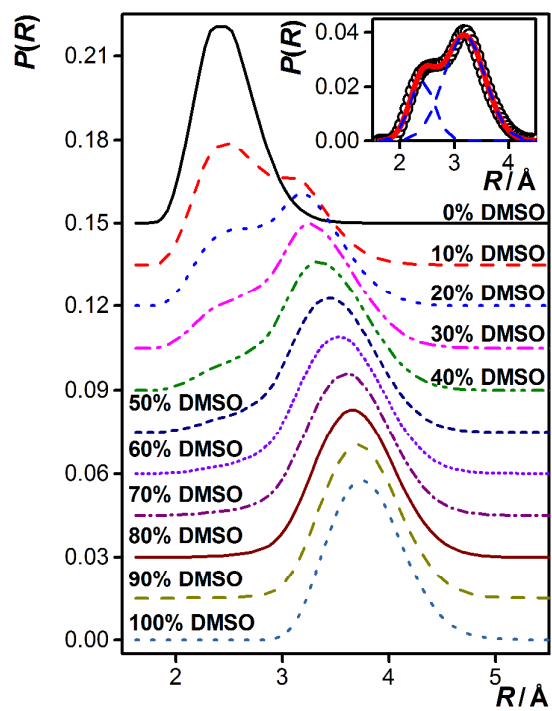
Figure 10.

Idrissi et al.
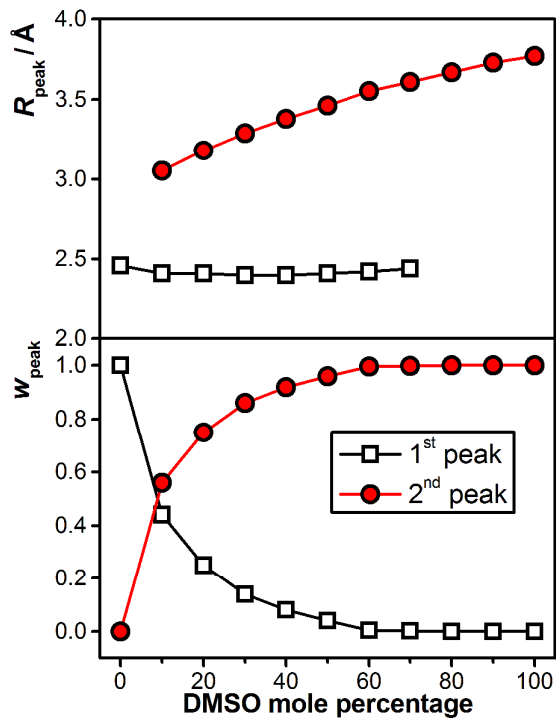
Figure 11.

Idrissi et al.
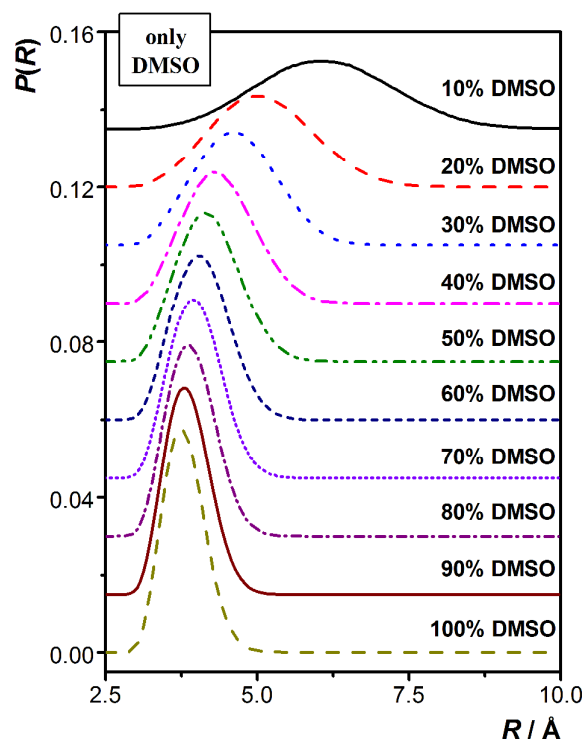
Figure 12.

Idrissi et al.

Figure 13.

Idrissi et al.